

## Research Article

# Nanocrystalline $\text{Pb}(\text{Zr}_{0.52}\text{Ti}_{0.48})\text{O}_3$ Ferroelectric Ceramics: Mechanical and Electrical Properties

**M. Venkata Ramana,<sup>1,2</sup> M. Penchal Reddy,<sup>2</sup> N. Ramamanohar Reddy,<sup>2</sup> K. V. Siva Kumar,<sup>2</sup> V. R. K. Murthy,<sup>3</sup> and B. S. Murty<sup>1</sup>**

<sup>1</sup>Nanotechnology Laboratory, Department of Metallurgical and Materials Engineering, Indian Institute of Technology, Madras, Chennai 600 036, India

<sup>2</sup>Ceramic Composite Materials Laboratory, Department of Physics, Sri Krishnadevara University, Anantapur 515 003, India

<sup>3</sup>Microwave Laboratory, Department of Physics, Indian Institute of Technology, Chennai 600 036, India

Correspondence should be addressed to M. Venkata Ramana, venkat6slr@gmail.com

Received 30 November 2009; Revised 24 February 2010; Accepted 22 March 2010

Academic Editor: Christian Brosseau

Copyright © 2010 M. Venkata Ramana et al. This is an open access article distributed under the Creative Commons Attribution License, which permits unrestricted use, distribution, and reproduction in any medium, provided the original work is properly cited.

Nanocrystalline powders of the composition  $\text{Pb}(\text{Zr}_{0.52}\text{Ti}_{0.48})\text{O}_3$  were obtained by Mechanical alloying (high-energy ball milling). X-ray diffraction studies show that these compounds are completely into the perovskite phase. Detailed studies of electrical and mechanical properties of PZT as a function of temperature (and frequency) showed the high permittivity of 20653 at Curie transition temperature. Temperature variation of longitudinal modulus and internal friction of these ceramics at 104 kHz frequency were studied in the wide temperature range of 30°C–420°C. The internal friction measurements showed sharp stress induced relaxation peaks in the present composition corresponding to those temperatures where the minima were noticed in temperature variation of longitudinal modulus behavior. This dielectric and internal friction behaviour was explained in the light of polaron hopping mechanism and structural phase transitions in the present piezoelectric compositions.

## 1. Introduction

In the preparation of nonvolatile memory devices, lead zirconate titanate (PZT) ceramics are very attractive for application as capacitor of dynamic random access memory (DRAM) and gate materials of ferroelectric RAM (FRAM). PZT materials are well known for their good piezoelectric properties and are ideal candidates for making sensors and actuators. The mechanical properties of PZT ceramics have received much less attention from researchers as compared to their electrical properties. Thus understanding of the mechanical properties of PZT has become important since these properties must be considered in the design of piezoelectric devices [1].

The solid solution of ferroelectric lead titanate ( $\text{PbTiO}_3$ ,  $T_c = 490^\circ\text{C}$ ) and antiferroelectric lead zirconate ( $\text{PbZrO}_3$ ,  $T_c = 230^\circ\text{C}$ ) abbreviated as PZT ( $\text{PbZr}_{1-x}\text{Ti}_x\text{O}_3$ ) with varying Zr/Ti ration is of great interest for many piezoelectric, pyroelectric, and ferroelectric devices. PZT

with  $x$  close to 0.48, near the morphotropic phase boundary between rhombohedral and tetragonal phases, has been considered very promising for piezoelectric devices [2]. Nanocrystalline ceramics can be synthesized by a various physical, chemical, and mechanical methods [3]. Recently, a mechanical alloying technique (i.e., high energy ball milling) has successfully been used to synthesize the nanocrystalline ferroelectric materials. Indeed, mechanical alloying was found to be superior to the high-temperature solid state reaction method/wet chemical process because it lowers the calcination and sintering temperature due to the nanocrystalline nature of the resultant powder. The properties of nanocrystalline materials are found superior to those of conventional polycrystalline coarse-grained materials. Mechanical alloying is very useful processes to prepare lead-based ceramics PZT, Lead Strontium Titanate (PST), and Lead Magnesium Neobate-Lead Titanate (PMN-PT) [4] because it takes place close to room temperature, then effectively alleviating the loss of  $\text{PbO}$ .

The properties of ferroelectrics largely depend on their domain structure geometry and nature of interaction of domain boundaries and various imperfections of their crystal lattice. The polycrystalline ferroelectrics have high concentration of point defects. Internal friction is very sensitive to the motion of point defects, domain walls, and other imperfections, so it has been used as an important tool to study the defects of the structure of ferroelectric materials for a long time. The internal friction in PZT (40-hour composition) was investigated in this study to give more information about the point defects and domain walls. In order to have a better understanding of the phase transitions and with smaller crystalline size, we have synthesized nanocrystalline PZT by mechanical alloying and measured dielectric, piezoelectric, longitudinal modulus ( $L$ ), and internal friction ( $Q^{-1}$ ) properties, on which, not much work has been reported so far.

## 2. Experimental Details

The PZT composition selected for this study was  $\text{Pb}(\text{Zr}_{0.52}\text{Ti}_{0.48})\text{O}_3$ , which is near the morphotropic phase boundary. The starting powders were  $\text{PbO}$  (97%),  $\text{ZrO}_2$  (98%), and  $\text{TiO}_2$  (99.9%). The oxide blend in the stoichiometric ratio was milled in planetary ball mill (Retsch PM 200) with tungsten carbide milling media (10 mm dia balls) at a ball-to-powder weight ratio of 10:1 and at a speed of 300 rpm. Milling was carried out in ethyl alcohol medium for a period of 10, 20, 30, and 40-hour. The milled powders were compacted uniaxially at 100 MPa to form pellets of the size 10 mm in diameter and 2 mm in thickness for dielectric and piezoelectric properties measurement. For measurement of longitudinal modulus and internal friction properties, bars of square cross-section with dimensions  $3.5 \text{ mm} \times 3.5 \text{ mm} \times 20.5 \text{ mm}$  were prepared using an uniaxial hydraulic press.

All the pellets and bars were calcined at  $700^\circ\text{C}$  for 2 hours and sintered at  $1100^\circ\text{C}$  for 2 hours in a closed alumina crucible. In order to prevent the  $\text{PbO}$  loss during high temperature sintering and to maintain desired stoichiometry, an equilibrium  $\text{PbO}$  vapour pressure was established with  $\text{PbZrO}_3$  as setter by placing pellets in a covered alumina crucible. The measured density of the sintered PZT pellets was found to be within 98-99% of its theoretical density. The phase identification was carried out using an X-ray diffractometer (Philips, PW-1710 XRD) with  $\text{CuK}\alpha$  radiation ( $\lambda = 0.15418 \text{ nm}$ ). Scanning electron microscopy (SEM, JEOL, JSM-5800) was employed to record and analyze the surface morphology of the ball milled powders and sintered pellets. The average crystalline size was calculated from the X-ray peak broadening using the vigot peak profile analysis [5] after eliminating the instrumental broadening and strain contribution, which was confirmed by the transmission electron microscopy (TEM) using a Philips CM 20 microscope.

The flat polished surfaces of the sintered pellets were electroded with high purity silver paint (Du Pont) and then dried at  $150^\circ\text{C}$  before making any electrical measurement. The capacitance and loss tangent ( $\tan \delta$ ) of the samples

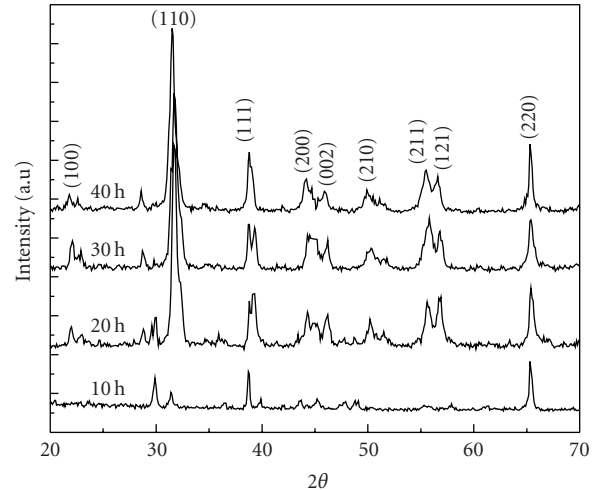


FIGURE 1: X-ray diffraction patterns of mechanically activated PZT ceramics at different milling times.

were measured with HIOKI-3535-50 LCR Hi tester under a weak electric field (with the maximum magnitude of 1 V) in the temperature range of 30 to  $500^\circ\text{C}$  at different frequencies. The piezoelectric coefficient ( $d_{33}$ ) was measured using a piezo  $d_{33}$  meter. The  $L$  and  $Q^{-1}$  of 40 hours milled sample were measured in the temperature range 30 to  $420^\circ\text{C}$  at  $5^\circ\text{C}$  intervals, in a tubular furnace. All the  $Q^{-1}$  and  $L$  measurements have been performed with strain amplitude of  $10^{-6}$ , after the specimen had attained thermal equilibrium.

The experimental technique employed in the present study for the measurement of internal friction and the longitudinal modulus was measured by using a composite oscillator technique [6]. From the resonant frequency ( $f_s$ ) of the composite system and the logarithmic decrement ( $\delta$ ), the  $Q^{-1}$  and the  $L$  have been evaluated using the standard relations as detailed in the literature [7, 8].  $Q^{-1}$  and  $L$  data obtained in the present work are accurate to  $\pm 5$  and  $\pm 2$ , respectively. The x-cut quartz transducer used in the present investigation has a length of 20 mm, width 33 mm, natural frequency 104 kHz and mass of 0.66 g. The electrode faces were painted with conducting silver paint. The composite oscillator was formed by cementing the quartz transducer to the specimen of identical cross-section. The adhesive used in the present work was a paste containing one part by weight of calcium carbonate and five parts by weight of sodium metasilicate in a small quantity of distilled water. In order to study the effect of temperature on internal friction and longitudinal modulus in the PZT specimen, the composite resonator system was placed at the centre of a tubular electrical furnace. The details of the furnace and temperature controller assembly were described elsewhere [6].

## 3. Results and Discussion

**3.1. Structural Characterization of PZT.** Figure 1 compares the XRD pattern of mechanical alloyed and sintered PZT pellets. Most of the XRD peaks of PZT were indexed in tetragonal and rhombohedral phases in the present systems

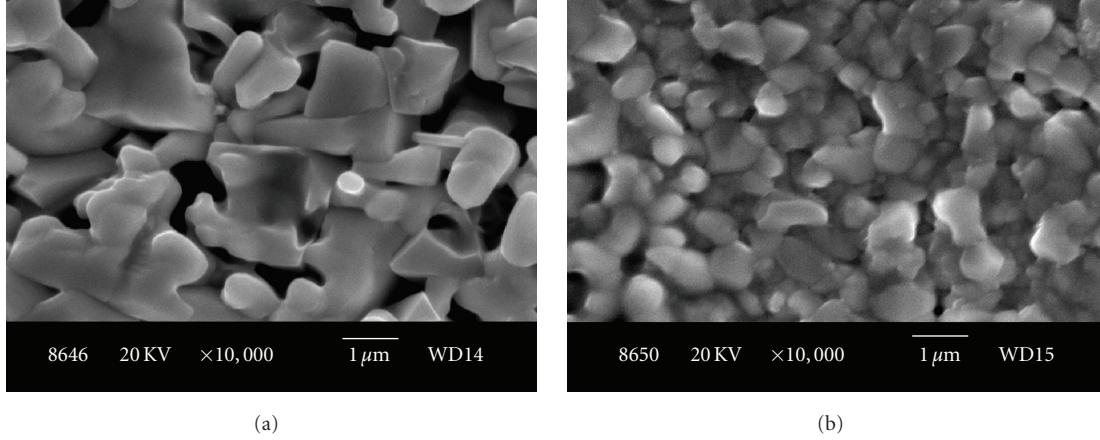


FIGURE 2: Scanning electron micrographs of PZT samples with 10 hours and 40 hours of milling time.

TABLE 1: Lattice parameters, density, dielectric constant at  $R_T$  and  $T_c$ , loss tangent  $d_{33}$  properties of PZT.

Parameters	Composition			
	10 hours	20 hours	30 hours	40 hours
$a$	3.9824	3.9844	3.9902	3.9976
$c$	4.0168	4.0125	4.0098	4.0013
$c/a$	1.0086	1.0070	1.0049	1.009
$\rho$	7.54	7.58	7.70	7.83
Crystallite size	45	42	41	38
$\epsilon$ at $R_T$	1244	1565	1654	1851
$\epsilon$ at $T_c$	14914	18207	18101	20652
$\delta$ at $R_T$	0.033	0.037	0.029	0.025
$d_{33}$	255	195	140	105

in different cell configuration and also formed completely into the perovskite structure after sintering at  $1100^\circ\text{C}$  for 2 hours. The indexing of XRD peaks and the determination of lattice parameters of PZT were carried out using a software package POWD [5]. On the basis of the best agreement between the observed and calculated  $d$  values of all the reflections, a unit cell of PZT was selected and its lattice parameters were refined using least-square subroutine of POWD. The refined lattice parameters are given in Table 1. The  $c/a$  ratios of the PZT formed by mechanical alloyed and sintered samples of different milling time were very close to each other, suggesting that the structure of the phase formed is the same irrespective of milling time. The crystallite size calculations using a single peak (101 of relative intensity  $I_p = 100$ ) of the sintered PZT show that it decreases from 45 to 38 nm on increasing the milling time. The decrease in the crystallite size results in a decrease of the tetragonal distortion. It is also noticed from X-ray diffractogram, that the most intensive peak (relative intensity  $I_p = 100$ ) of the diffractogram has regular shift towards lower  $2\theta$  value with decrease in crystallite size.

Figures 2(a) and 2(b) show the morphology and size distribution of milled and sintered PZT pellets. The particles are more or less spherical in this morphology. The individual

particle observed in the SEM is expected to be polycrystalline and hence their size is larger than the crystallite size obtained in X-ray peak broadening. The particle size gradually decreases with increasing milling time and was found to be in the range of 0.5 to  $1\ \mu\text{m}$ . Figure 3 shows the bright field electron micrograph of the 40-hour milled sample, the inset shows a selected area diffraction patterns which clearly established the nanocrystalline nature of the PZT.

In TEM studies (Figure 3), it was observed that when the electron beam strikes the polycrystalline agglomerated particles (as observed in SEM studies), the agglomerates disintegrate leading to a sea of individual nano crystalline particles, each one of them being a single crystalline particle. The size of these particles is found to be in the range of 20 nm, which is comparable to the crystallite size calculations (10 nm) based on the XRD peak broadening.

It is also observed that the higher milling time and sintered PZT show small particle size. Sintering parameters have a strong influence on the electrical properties on the PZT ceramics. In general, electrical properties of ferroelectric ceramics increase with the increasing grain size [9, 10]. This is not true in the present study because of fine particles. The particle size of PZT decreases with increase in milling time, which results in improved dielectric constant. The particle size affects the electrical properties mainly by restricting the domain-wall switching. A space-charge model of ferroelectric ceramics indicates that the space charge field, which influences the domain switching, decreases with increasing grain size.

**3.2. Electrical Properties.** The temperature dependence of dielectric behavior of milled and sintered PZT samples with milling time is presented in Figure 4. It can be observed that in all the cases, the dielectric constant increases and reaches a maximum value  $\epsilon_{\text{max}}$  (at  $T_c$ ) and then decreases with further increase in temperature. The dielectric peak is broad, which is a general feature of ferroelectric materials. The dielectric constant of PZT at  $T_c$  was found to be 14914, 18207, 18101, and 20652 for 10, 20, 30, and 40 hours mechanical activated PZT, respectively. Whereas the hand ground PZT



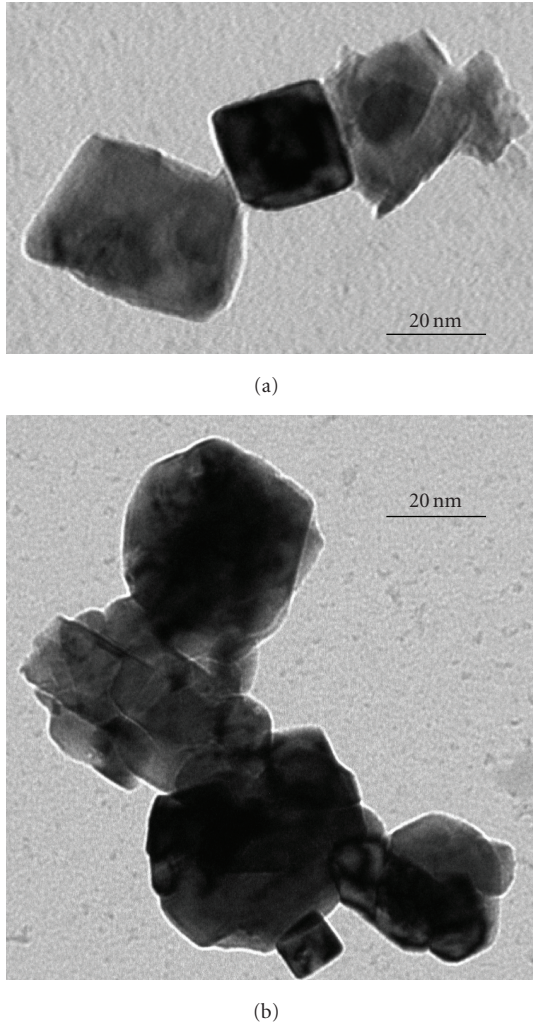


FIGURE 3: Transmission electron micrographs of PZT samples with 30 hours and 40 hours of milling time.

shows only 6763 at Curie transition temperature. The  $T_c$  does not show significant variation with milling time and is 396°C in all the samples. Figures 5(a) and 5(b) show the variation of dielectric constant with milling time at room temperature and  $T_c$  for these samples. It reveals that the dielectric constant increases with increase of milling time in both cases. This indicates that the PZT prepared by MAS is superior to that prepared by high temperature solid state reaction method. Dielectric constant (at room temperature and curie transition temperature) as a function of crystalline size of the MAS prepared PZT was shown in Figure 6. It reveals that, the room temperature and Curie transition temperature dielectric property increase with decreasing the crystalline size. At lowest crystalline size, it gives the highest magnitude of dielectric property.

The variation of  $\tan \delta$  with temperature for the PZT samples is presented in Figure 7. It can be observed from Figure 7, that all the PZT samples show a significant increase in  $\tan \delta$  at higher temperature. The increase in tangent loss ( $\tan \delta$ ) is attributed to an increase in the conduction of

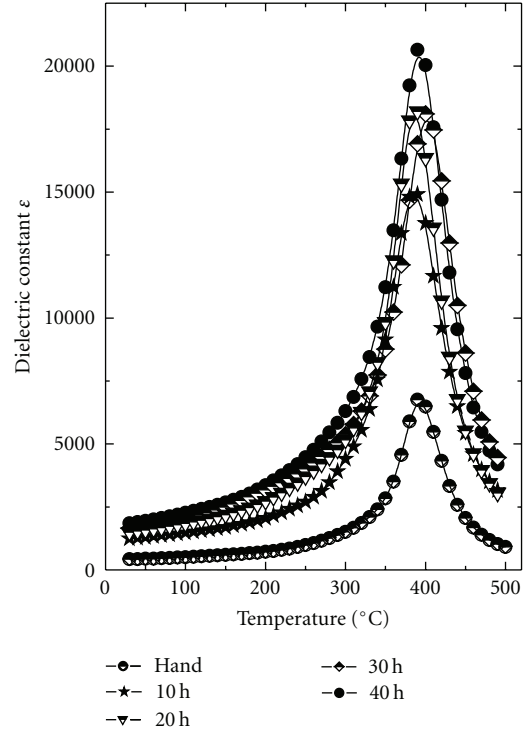


FIGURE 4: The dielectric constant ( $\epsilon$ ) versus Temperature of PZT with milling time.

residual current and absorption current. The tangent loss caused by the dipole movement reaches its maximum at a certain definite temperature. In fact, the rise in temperature and the resulting drop in viscosity exert a double effect on the amount of losses due to the friction of the rotating dipoles. The degree of the dipole orientation increases, and at the same time, there is a reduction in the energy required to overcome the resistance of the viscous medium (internal friction matter) when the dipole rotates through a unit angle. The first factor increases  $P_s$  (spontaneous polarization) and therefore the tangent loss and the second factor decrease these magnitudes. Apart from the dipolar losses, the losses due to the electrical conduction, which increase with an increase in temperature, are also shown in Figure 6.

For piezoelectric coefficient ( $d_{33}$ ) measurements, each sample was poled at 150°C for 2 hours in silicon oil bath, which allows higher poling fields than those used in air due to the increase in breakdown voltage, and then cooled to room temperature with continuously applied electric field and as a result this gives a balanced poling processes to enable observations of any change in piezoelectric properties of poling levels [11]. Table 1 depicts the trend of  $d_{33}$  values of mechanical-activated synthesized PZT samples. It is found that as the milling time increases, the piezoelectric coefficient,  $d_{33}$ , decreases gradually, due to the particles reduced submicron size with increasing the milling time, which is evident in the scanning electron micrographs (Figure 2).

**3.3. Mechanical Properties of Pure PZT.** In order to determine the critical behavior in the phase transition region and the

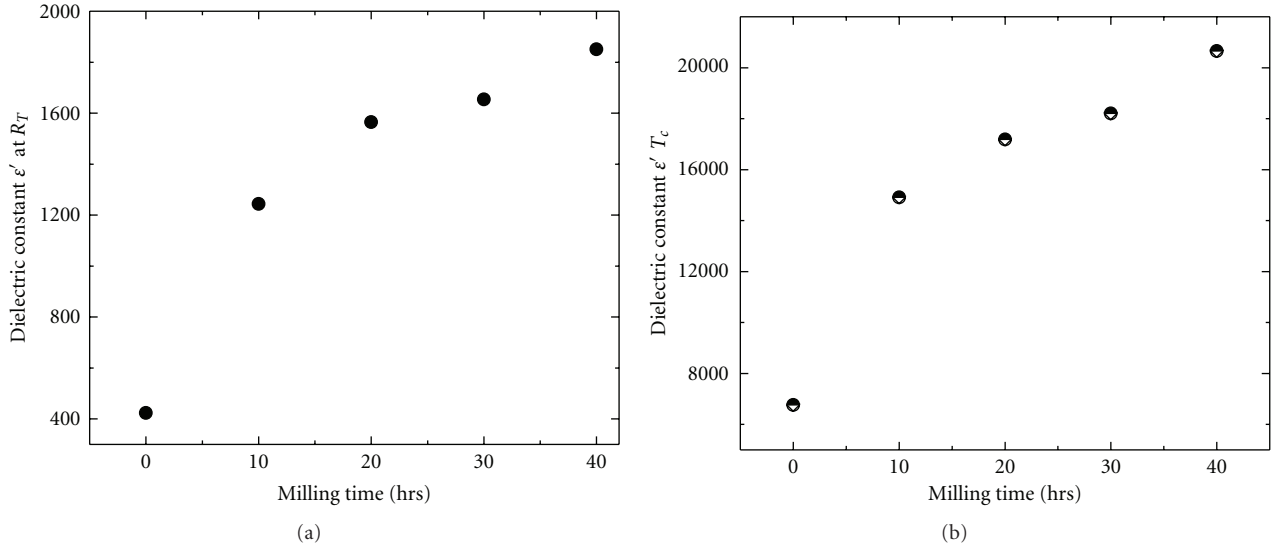


FIGURE 5: Variation of dielectric constant with milling time at (a) room temperature and (b)  $T_c$ .

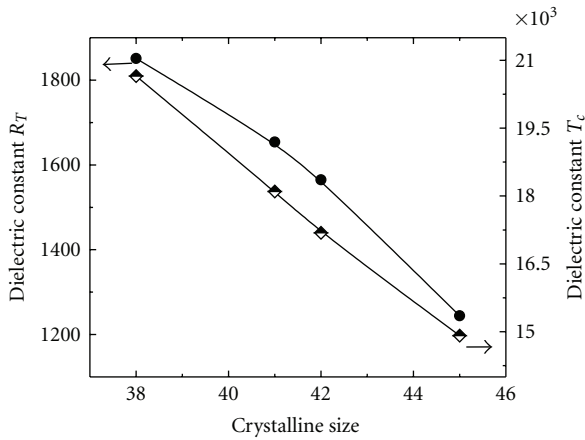


FIGURE 6: The dielectric properties ( $R_T$  and  $T_c$ ) as a function of crystalline size.

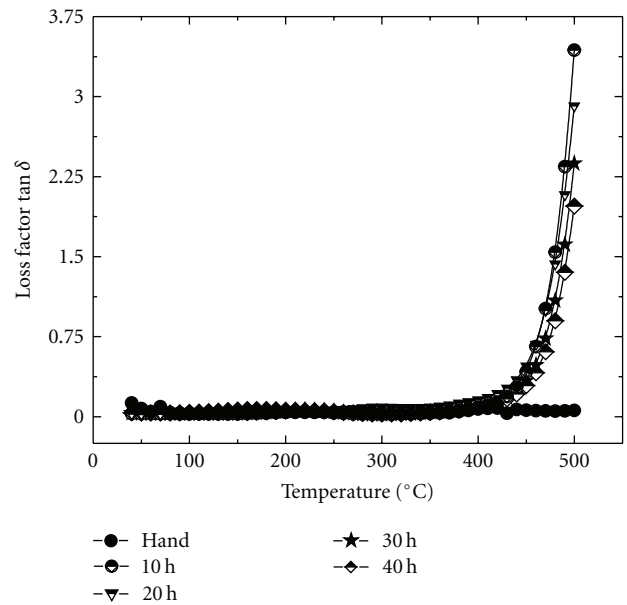


FIGURE 7: The dielectric loss factor  $\tan \delta$  of PZT prepared with different milling times.

extrinsic contributions to the elastic modulus and internal friction measurements were carried out on both sides of the transition temperature, avoiding outside disturbances that could cause most anomalies within the material itself. Internal friction is a very sensitive property to the microstructure of the materials, especially to the point defects, oxygen ion vacancies, and domain wall motions. Many studies, related to the oxygen vacancies [12], domain walls [13] and phase transitions [14] in ferroelectric ceramics have been performed by the means of internal friction measurements. The internal friction of PZT was first reported by Postnikov et al., [12] where two internal friction peaks are observed, located around  $140^{\circ}\text{C}$  and  $240^{\circ}\text{C}$ , respectively and these are attributed to the interaction of point defects and domain wall. Recently Bourim et al., [15] observed two internal

friction peaks in  $\text{PbZr}_{0.52}\text{Ti}_{0.48}\text{O}_3$  at  $375^{\circ}\text{C}$  and  $69^{\circ}\text{C}$  at low frequencies. Dai et al. [16] also observed two low temperature internal friction peaks for the same piezoelectric ceramic  $\text{PbZr}_{0.52}\text{Ti}_{0.48}\text{O}_3$  at 261 k and 255 k at low frequencies. But Chen et al., [17] observed only one internal friction peak near the Curie transition temperature. Not much was done on PZT at high frequency side, so far.

In this work, the experimental results on internal friction and longitudinal modulus are reported at high frequency by the means of composite oscillator technique. PZT sample milled for 40 hours was chosen for  $Q^{-1}$  and  $L$  measurements

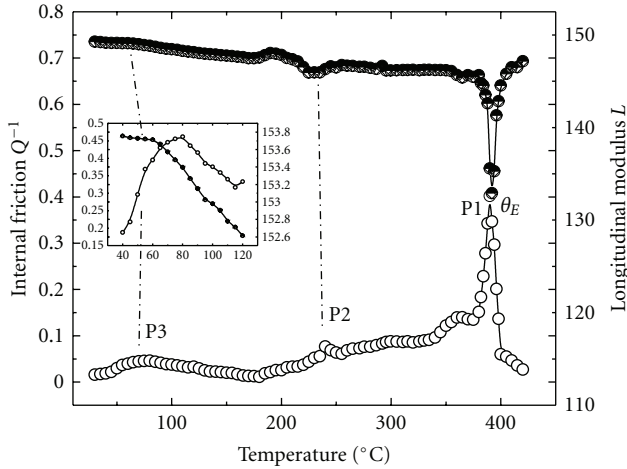


FIGURE 8: Temperature variation of internal friction and longitudinal modulus of PZT (40 hours sample).

as it posses high dielectric constant at room temperature and at  $T_c$  and also a low loss tangent. These measurements were made in the temperature range 30 to 420°C at higher fixed frequency in the interval of 5°C. In the real ferroelectrics, the domain boundary movement is limited by the different crystal lattice imperfections such as interstitial atoms, vacancies, and dislocations. The point defects, for example, may play the role of stoppers for domain boundaries and point defects can result in the hysteresis losses due to unpinning at domain boundaries. Therefore, the interaction of point defects with the domain boundaries which leads to the internal friction is of great interest. The temperature dependence of internal friction and longitudinal modulus for a PZT ceramic sample has been measured at 104 kHz during heating process as shown in Figure 8. Three internal friction peaks (P1, P2 and P3) appear around 392°C, 240°C, and near to 100°C, respectively. In the temperature range around the internal friction peaks, the relative longitudinal modulus of the specimen decreases with increasing temperature. According to the phase diagram [2], the P1 and P2 are due to the Curie transition temperature between paraelectric and ferroelectric phase, and the morphotropic phase transition between rhombohedral and tetragonal ferroelectric phases, respectively. This type of anomalies behaviour was reported earlier by Jamenez and Vicente [18] and Grindnev et al., [19] in niobium doped PZT ceramics and Bourim et al., [15] in pure PZT.

The peak P1 appears around 392°C; it is  $\theta_E$  and the peak P2 appeared around 240°C was attributed to the movement of domain walls and point defects in the sample. In other words, the density of domain walls increases when the temperature approaches the Curie point. The increment of the mobility and density of domain walls result in an increase of internal friction. When the density of domain walls is so great that the interaction between walls affects the mobility of the walls strongly, the internal friction decreases, then forming an internal friction peak. The resonant frequency minimum is due to the modulus defect as a result of domain wall motion. The P2 peak dependence on the torsion stress

amplitude could be explained by the interaction between ferroelectric domain walls and oxygen vacancies and the drag of the vacancies to the movement of domain walls and perhaps their pinning such as in Granato and Lucke theory for dislocation pinning [20]. The P2 peak is controlled by the superposition of viscous motion of domain walls and the interaction between domain walls and the oxygen vacancies. The fact that the P2 peak is a superposition of two peaks can be verified also by the comparison of the P2 peak fitted with Gaussian model [21] to a simple Debye peak, and from the calculation of the widening factor as shown by Schaller et al. [22]. Temperature variation of internal friction and modulus of PZT revealed one more broad peak and kink at low temperature around 80 and 65°C, respectively, is shown in Figure 7 (inset). This low temperature peak is related to oxygen vacancies-which may be introduced into the PZT by loss of PbO in the specimen synthesis and probably cation vacancies (Zr,Ti) [23]. This low temperature peak is a broadened Debye in nature. This internal friction has the characteristic of a static hysteresis type. To explain that, we suppose that the P3 peak is due to the formation of anisotropic anelastic dipoles between oxygen vacancy and cation ion. These dipoles present a low symmetry compared to the whole crystal lattice. The reorientation of the dipole can take place by the jump of the vacancy around the cation ion under the applied torsion stress, resulting in mechanical relaxation, whereas an isolated vacancy do not give place to any relaxation.

Generally, in ferroic materials, the density of domain walls increases when the temperature approaches the Curie transition temperature. With the increase in temperatures the increase of mobility and density of domain walls results in an increase of the internal friction. If the density of domain walls is very large, the interaction of domain walls affects the mobility of domain walls; the internal friction decreases. These two opposing tendencies lead to the formation of internal friction peak. The broad peak could be attributed to the interaction of 90° domain walls with Ti or Zr vacancies. This hypothesis is confirmed by the decrease of the broad peak due to the reduction of the Ti or Zr vacancies by introducing niobium Nb<sub>2</sub>O<sub>5</sub> in PZT (Nb replaces Ti or Zr atoms) as observed by Postnikov et al., [12]. Thus, the broad peak could be related to the viscous motion of domain walls due to the interactions of point defects with domain walls whose microstructure evolves with temperature and stress amplitude. Moreover, the domain walls from oxygen vacancies can be further supported, since the broad peak shape underwent some variation at the time the oxygen vacancy concentration and mainly induced by the loss in PbO. Therefore, we can deduce that the broad peak is directly related to the grain size although it is attributed to the motion of domain walls. The peak around 230°C disappeared in the ferroelectric ceramics with smaller grain size, because of the strong pinning effect that grain boundaries exert on the domain walls [24]. In the absence of any phase transition, generally in solids, the elastic modulus decreases with the increase in temperature. However, in the present investigation, the PZT transforms from ferroelectric to the nonferroelectric phase at 390°C. Hence, there should be

anomalous behavior in both elastic and anelastic properties near the phase transition, because these are lattice-related properties.

#### 4. Conclusions

PZT with the composition  $\text{PbZr}_{0.52}\text{Ti}_{0.48}\text{O}_3$  was prepared by mechanical alloying. All these patterns depict the formation of the phase with tetragonal and rhombohedral structures, also formed completely into the perovskite structure. The result also clearly shows that there are no diffraction peaks from impurity phases. The particles are more or less spherical in its morphology. The individual particle observed in the SEM is expected to be polycrystalline and hence their size is larger than the crystallite size obtained in X-ray peak broadening. The size of these particles (in TEM) was found to be in the range of 20 nm, which is comparable to the crystallite size calculations (10 nm) based on the XRD peak broadening. The particle size gradually decreases with increasing milling time. The dielectric constant increased with increasing milling time (decreases in crystalline size) and reached a value of 20,653 at  $T_c$  at 100 kHz. In contrast, the  $d_{33}$  value decreased with the increase in milling time.

The internal friction corresponding to longitudinal modulus with the variation of temperature shows three peaks. The high-temperature peak which appears near the Curie transition temperature (between ferroelectric and paraelectric phases) originates from the viscous movement of domain walls. The low temperature peak is a broadened Debye peak in nature and it is attributed to the oscillation damping of the domain walls acted by the changed oxygen vacancies. There is another peak around 240°C, in between 90°C and 392°C; it is caused by the relaxation of oxygen vacancy clusters near the 90° domain walls. This peak is due to the superposition of the viscous motion of domain walls and point defects (oxygen vacancies-cationic vacancies). The longitudinal modulus versus temperature measurements allows us to determine easily the phase transition temperatures. All our results show good agreement with data from the literature.

#### References

- [1] B. W. Chua, L. Lu, M. O. Lai, and G. H. L. Wong, "Effects of complex additives on toughness and electrical properties of PZT ceramics," *Journal of Alloys and Compounds*, vol. 381, no. 1-2, pp. 272–277, 2004.
- [2] B. Jaffe, W. R. Cook, and H. Jaffe, *Piezoelectric Ceramic*, Academic, London, UK, 1971.
- [3] S. K. S. Parashar, R. N. P. Choudhary, and B. S. Murty, "Electrical properties of Gd-doped PZT nanoceramic synthesized by high-energy ball milling," *Materials Science and Engineering B*, vol. 110, no. 1, pp. 58–63, 2004.
- [4] L. B. Kong, J. Ma, W. Zhu, and O. K. Tan, "Preparation of PMN-PT ceramics via a high-energy ball milling process," *Journal of Alloys and Compounds*, vol. 336, no. 1-2, pp. 242–246, 2002.
- [5] H. P. Klug and L. Alexander, *X-Ray Diffraction Procedure for Polycrystalline and Amorphous Materials*, John Wiley & Sons, New York, NY, USA, 2nd edition, 1974.
- [6] N. Ramamanohar Reddy, M. Venkata Ramana, K. Krishnaveni, K. V. Siva Kumar, and V. R. K. Murthy, "Dielectric, elastic, anelastic and conductivity behaviour of ferroelectromagnetic composites,  $\text{Ni}_{0.5}\text{Zn}_{0.5}\text{Fe}_{1.95}\text{O}_{4-\delta} + \text{Ba}_{0.8}\text{Pb}_{0.2}\text{TiO}_3$ ," *Bulletin of Materials Science*, vol. 30, no. 4, pp. 357–363, 2007.
- [7] J. Marx, "Use of the piezoelectric gauge for internal friction measurements," *Review of Scientific Instruments*, vol. 22, no. 7, pp. 503–509, 1951.
- [8] W. H. Robinson and A. Edgar, "The piezoelectric method of determining mechanical damping at frequencies of 30 to 200 kHz," *IEEE Transactions on Sonics and Ultrasonics*, vol. 21, no. 2, pp. 98–105, 1974.
- [9] K. Okazaki and K. Nagata, "Effects of grain size and porosity on electrical and optical properties of PLZT ceramics," *Journal of the American Ceramic Society*, vol. 56, no. 2, pp. 82–86, 1973.
- [10] C. A. Randall, N. Kim, J.-P. Kucera, W. Cao, and T. R. ShROUT, "Intrinsic and extrinsic size effects in fine-grained morphotropic-phase-boundary lead zirconate titanate ceramics," *Journal of the American Ceramic Society*, vol. 81, no. 3, pp. 677–688, 1998.
- [11] M. Venkata Ramana, N. Ramamanohar Reddy, G. Sreenivasulu, K. V. Siva Kumar, B. S. Murty, and V. R. K. Murthy, "Enhanced magnetoelectric voltage in multiferroic particulate  $\text{Ni}_{0.83}\text{Co}_{0.15}\text{Cu}_{0.02}\text{Fe}_{1.9}\text{O}_{4-\delta}/\text{PbZr}_{0.52}\text{Ti}_{0.48}\text{O}_3$  composites—dielectric, piezoelectric and magnetic properties," *Current Applied Physics*, vol. 9, no. 5, pp. 1134–1139, 2009.
- [12] V. S. Postnikov, V. S. Pavlov, and S. K. Turkov, "Internal friction in ferroelectrics due to interaction of domain boundaries and point defects," *Journal of Physics and Chemistry of Solids*, vol. 31, no. 8, pp. 1785–1791, 1970.
- [13] Y. N. Wang, W. Y. Sun, X. Y. Chen, H. M. Shen, and B. S. Lu, "Internal friction associated with the domain walls and the second-order ferroelastic transition in LNPP," *Physica Status Solidi (a)*, vol. 102, no. 1, pp. 279–285, 1987.
- [14] B. L. Cheng, M. Gabbay, W. Duffy Jr., and G. Fantozzi, "Mechanical loss and Young's modulus associated with phase transitions in barium titanate based ceramics," *Journal of Materials Science*, vol. 31, no. 18, pp. 4951–4955, 1996.
- [15] E. M. Bourim, H. Tanaka, M. Gabbay, and G. Fantozzi, "Internal friction and dielectric measurements in lead zirconate titanate ferroelectric ceramics," *Japanese Journal of Applied Physics, Part 1*, vol. 39, no. 9B, pp. 5542–5547, 2000.
- [16] Y. R. Dai, P. Bao, H. M. Shen, et al., "Internal friction study on low-temperature phase transitions in lead zirconate titanate ferroelectric ceramics," *Applied Physics Letters*, vol. 82, no. 1, pp. 109–111, 2003.
- [17] X. B. Chen, C. H. Li, Y. Ding, et al., "Dielectric relaxation and internal friction related to the mobility of domain wall in PZT ferroelectrics," *Physica Status Solidi (a)*, vol. 179, no. 2, pp. 455–461, 2000.
- [18] B. Jamenez and J. M. Vicente, "The low-frequency young modulus and internal friction in Pb-Ca and Pb-Zr titanate ceramics," *Journal of Physics D*, vol. 31, no. 1, pp. 130–136, 1998.
- [19] S. A. Grindnev, B. M. Darinskii, and V. S. Postnikov, *Bulletin of the Academy of Sciences of the USSR*, English translation in *Physical Science*, vol. 33, p. 1106, 1969.
- [20] A. Granato and K. Lücke, "Theory of mechanical damping due to dislocations," *Journal of Applied Physics*, vol. 27, no. 6, pp. 583–593, 1956.
- [21] A. Bouzid, M. Gabbay, and G. Fantozzi, "Potassium doping effect on the anelastic behaviour of lead zirconate titanate—PZT—near to the morphotropic phase boundary," *Diffusion and Defect Data. Part A*, vol. 206–207, pp. 147–150, 2002.



- [22] R. Schaller, G. Fantozzi, and G. Gremaud, *Mechanical Spectroscopy  $Q^{-1}$* , Tran Tech, Zurich, Switzerland, 2001.
- [23] H. Frayssignes, M. Gabbay, G. Fantozzi, N. J. Porch, B. L. Cheng, and T. W. Button, "Internal friction in hard and soft PZT-based ceramics," *Journal of the European Ceramic Society*, vol. 24, no. 10-11, pp. 2989–2994, 2004.
- [24] C. Wang, Q. F. Fang, and Z. G. Zhu, "Internal friction study of  $\text{Pb}(\text{Zr}, \text{Ti})\text{O}_3$  ceramics with various Zr/Ti ratios and dopants," *Journal of Physics D*, vol. 35, no. 13, pp. 1545–1549, 2002.